



ELSEVIER

Physica C 228 (1994) 175–180

PHYSICA C

Magnetotransport in single-crystal Rb_3C_{60}

J.G. Hou *, X.-D. Xiang, Vincent H. Crespi, Marvin L. Cohen, A. Zettl

*Department of Physics, University of California at Berkeley, and
Materials Sciences Division, Lawrence Berkeley Laboratory, Berkeley, CA 94720, USA*

Received 3 May 1994

Abstract

The electrical resistivity of single-crystal Rb_3C_{60} has been measured in magnetic fields up to 7.0 T. A substantial broadening of the resistive transition to the superconducting state is observed and attributed to the combined effects of magnetofluctuations near T_c and thermally activated flux creep dominant at lower temperatures. We evaluate characteristic parameters for Rb_3C_{60} crystals including the upper critical field $H_{c2}(T)$, the scattering time τ , coherence length ξ , and mean free path l ; these are contrasted to similar parameters determined previously for K_3C_{60} .

1. Introduction

Compounds based on C_{60} represent a new class of molecular solids with interesting and unique structural and electronic properties. With suitable alkali-metal doping, C_{60} becomes superconducting with surprisingly high transition temperatures T_c [1,2]. Of the materials with a single type of alkali-metal dopant, Rb_3C_{60} has the highest T_c , about 30 K. Both unconventional and conventional mechanisms have been suggested to account for the superconductivity. Recently it was demonstrated that K_3C_{60} and Rb_3C_{60} can be synthesized as bulk, strictly three-dimensional superconductors [3]. Such specimens are ideal for the evaluation of intrinsic normal-state and superconducting parameters, including the behavior in a finite magnetic field. Previous measurements of upper critical fields $H_{c2}(T)$ of Rb_3C_{60} used powder polycrystalline samples and yielded extrapolated zero temperature values $H_{c2}(0)$ from 46 T to 78 T [4–6].

We report here the study of the electronic-transport properties of Rb_3C_{60} single crystals in magnetic fields. In contrast to the behavior observed for K_3C_{60} [7], we find that the resistive transition near T_c is substantially broadened by application of a magnetic field, a situation similar to high- T_c oxide superconductors. This broadening necessitates a detailed treatment of the resistive transition in order to extract accurate values of $T_c(H)$. Simply defining T_c as the onset or halfway point of the resistive transition yields incorrect values for T_c when the transition has significant width. In analogy to high- T_c oxide superconductors, we consider two mechanisms which contribute to the finite transition widths, thermodynamic fluctuations [8] and dissipative flux-line motion [9]. Our results suggested that near the transition onset the anomalous broadening is dominated by fluctuation magnetoconductivity, while at lower temperatures the dissipation is dominated by flux creep with a characteristic activation energy substantially lower than that found for conventional superconductors. We use the analysis of fluctuation magnetoconductivity to determine the thermodynamic T_c and thereby accurately determine the upper critical

* Corresponding author. Present address: Dept. of Chemistry, Oregon State University, Corvallis, OR 97331-4003, USA.

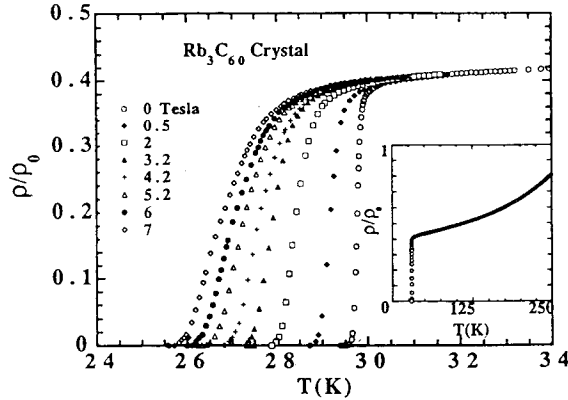


Fig. 1. Electrical resistivity vs. temperature for Rb_3C_{60} in different magnetic fields H . Inset: Resistivity for $H=0$.

field $H_{c2}(T)$ and the Ginzburg–Landau coherence length $\xi(0)$. The analysis also provides an estimate of the zero-temperature scattering time τ , the mean free path l and the penetration depth $\lambda(0)$.

2. Experimental

High-quality C_{60} single crystals were prepared by vapor transport and characterized by X-ray diffraction. Rb doping was performed using a procedure similar to that used for K_3C_{60} [10]. The electrical resistivity was measured using a DC four-probe Van der Pauw configuration.

3. Results

The inset to Fig. 1 shows the resistivity ρ of Rb_3C_{60} measured over a wide temperature range for $H=0$. A metallic temperature dependence is observed. The two components of the Van der Pauw resistance can be fitted to the same heuristic functional form of temperature dependence ($\rho = \rho_0 + AT^2$), indicating good sample homogeneity. The transition to the superconducting state is sharp with a transition width less than 200 mK. The main body of Fig. 1 shows the resistive transition for different H . Application of the field reduces T_c and broadens the resistive transition. Measurements on different samples yield similar results indicating that the broadening is intrinsic. Definition of $T_c(H)$ as the onset of the resistive transition yields values of $dH_{c2}(T)/dT$ and the upper critical-field curve

$H_{c2}(T)$ which are very different from those obtained by defining T_c as the halfway point of the resistive transition. For example, onset T_c 's yield $dH_{c2}(T)/dT = (-4.04 \text{ T/K})$ whereas halfway point T_c 's yield (-3.14 T/K) . It is clear that a detailed analysis of magnetoresistance data is necessary in order to extract intrinsic thermodynamic transition temperatures.

4. Discussion

4.1. Thermodynamic fluctuation of magnetoconductivity above T_c

We first investigate the origin of the magnetic field-induced broadening for the upper portion of the resistive transition in Rb_3C_{60} . It has been previously demonstrated [3] that in the absence of a magnetic field, Rb_3C_{60} displays fluctuation conductivity effects above T_c , with $\sigma' \propto t^{-1/2}$, where σ' is the excess fluctuation conductivity and $t = (T - T_c)/T_c$ is the reduced temperature. This is the behavior expected for a bulk three-dimensional superconductor. For finite magnetic field, the divergence of the fluctuation conductivity is expected to shift to a lower T_c due to pair breaking, leading to an H dependence of σ' . In addition, the fluctuation conductivity should become anisotropic. For a bulk superconductor in the dirty limit and for H parallel to the DC electrical current density J , the excess conductivity in the high-field limit becomes [11] $\sigma'_{\parallel} = AH^{1/2}t^{-3/2}$, similar to the result for one-dimensional filaments (the allowed states in momentum space are cylinders in both cases). When H is perpendicular to J , $\sigma'_{\perp} = BTH^{-1/2}t^{-1/2}$ as for $H=0$ [11]. Our crystals are roughly $0.5 \times 0.5 \times 0.1 \text{ mm}^3$, with the magnetic field oriented approximately perpendicular to the crystal surface.

Because the conductivity is measured in a Van der Pauw configuration, the excess conductivity will include both parallel and perpendicular contributions. Consequently, we expect a magnetic field-dependent fluctuation conductivity $\sigma' = \sigma'_{\perp} + \sigma'_{\parallel} = \sigma(T) - \sigma_n$, where σ_n is the normal-state conductivity (which has a linear temperature dependence near T_c [3]).

We fit the excess conductivity above T_c with the form $\sigma' = AH^{1/2}t^{-3/2} + BTH^{-1/2}t^{-1/2}$, where A and B are fitting parameters for all temperatures and fields and $T_c(H)$ is taken as an adjustable fitting parameter for

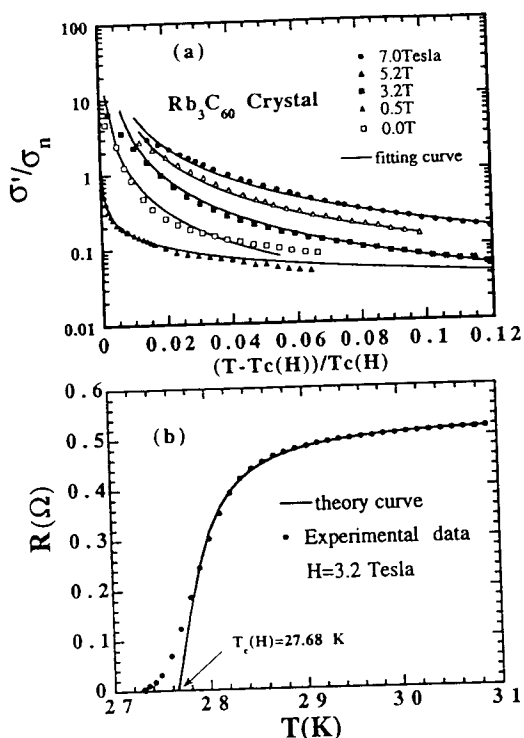


Fig. 2. (a) Normalized excess fluctuation conductivity vs. reduced temperature for Rb_3C_{60} in different magnetic fields. The solid lines are fits to $\sigma' = AH^{1/2}t^{-3/2} + BTH^{-1/2}t^{-1/2}$ (see text) with fitting parameters $A = 1.23 \times 10^{-4}$ and $B = 5.5 \times 10^{-5}$. (b) Resistance vs. temperature at $H = 3.2$ T. The solid line is a fit to the fluctuation conductivity formula (see text).

different fields. Fig. 2a shows the best fits thus obtained; with $A = 1.23 \times 10^{-4}$ and $B = 5.5 \times 10^{-5}$. They are in good agreement with the experimental data over a wide range of reduced temperature t . Fits to the fluctuation conductivity expression allow the field-dependent transition temperature $T_c(H)$ to be accurately determined. Fig. 2(b) shows in detail the resistive transition for $H = 3.2$ T, along with the calculated magnetofluctuation curve. $T_c(H = 3.2$ T) is indicated in the figure. We use $T_c(H)$ thus determined to extract $H_{c2}(T)$. However, before turning to a discussion of $H_{c2}(T)$, we first investigate a second dissipation mechanism which is dominant in the lower portion of the resistive transition.

4.2. Flux-creep resistance at low temperatures

The quality of the fluctuation conductivity fit in Fig. 3(b) is excellent for the high-temperature data shown in the figure, but degrades for lower temperatures. The

low-temperature deviation is suggestive of an additional dissipation mechanism involving dissipative flux-line motion. For a type-II superconductor in the mixed state, one expects dissipation due to flux creep at low temperatures [12,13]. The theory of flux creep by Anderson and Kim [12] assumes thermally activated jumps of flux lines at the rate given by $\nu = \nu_0 \exp(-U/k_B T)$, where U is the activation energy corresponding to the barrier height of the flux-line potentials. In the conventional expression for flux creep [14], the resistivity is

$$\rho = \frac{2\nu_0 LH}{J} \exp\left(-\frac{U}{k_B T}\right) \sinh\left(\frac{JHV_c L}{k_B T}\right), \quad (1)$$

where ν_0 is the attempt frequency of flux lines or bundles over a pinning barrier, U is the pinning barrier height, L is a hopping distance, and V_c is the volume of one vortex. Assuming the hopping distance L equals the inter-vortex distance a_0 , we find $V_c L \cong a_0^3 L_c$ (where L_c is the flux-line length). In our experiment, the current density is very small ($J \approx 0.2$ A/cm²), so the sinh term in Eq. (1) can be linearized, yielding

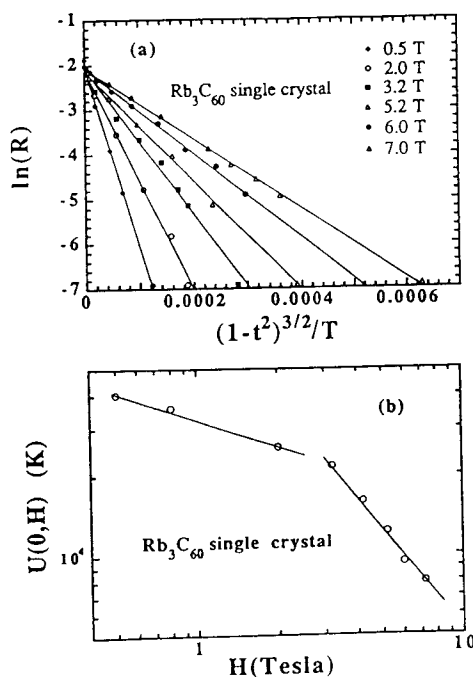


Fig. 3. (a) $\ln(R)$ vs. $(1-t^2)^{3/2}/T$ in the flux creep regime. The solid lines are fits to Eq. (2). (b) Field dependence of activation energy $U(0, H)$. The solid lines are fits to a power-law behavior, $U_0 \propto H^{-m}$, with $m = 1.25$ for $H > 3$ T, and $m = 0.35$ for $H < 2$ T.

$$\rho \approx (2\nu_0 \Phi_0^2 L_c / k_B T) \exp(-U/k_B T)$$

$$= \rho_c \exp(-U/k_B T), \quad (2)$$

where $\Phi_0 = Ha_0^2$ is the flux quantum. Previous theoretical and experimental studies [14–16] on flux creep of high- T_c superconductors have indicated that the activation energy U in Eq. (2) is often temperature- and field-dependent. We assume here that U has a simple scaling form with field H and normalized temperature $t' = T/T_c(H)$ [17]: $U(T, H) = U(H)(1 - t'^2)^{3/2}$, where $U(H)$ is the field-dependent activation energy. The prefactor ρ_c in Eq. (2) depends weakly on temperature and in our temperature region of interest (29 K to 26 K) ρ_c may be taken as a constant. In Fig. 3(a) we replot the low-temperature magnetoresistance data for Rb_3C_{60} as $\ln(R)$ versus $(1 - t'^2)^{3/2}/T$, where R is the sample resistance. The solid lines are linear fits to the data. The results show clearly that the data are well accounted for by Eq. (2) with a unique ρ_c . Fig. 3(b) shows $U(H)$ versus H . If a power law form for the field dependence of the activation energy is assumed, $U(H) = A/H^m$, then two field regimes become apparent, as indicated in Fig. 3(b). For H below 2 T, $m = 0.32$; while for H larger than 3 T, $m = 1.25$.

We emphasize two salient features of the flux creep dissipation in Rb_3C_{60} . First, in the temperature and field regime of our experiment, the activation energies are less than 1 eV. For conventional superconductors the activation energies are typically several eV. Second, the ratio of the prefactor ρ_c ($-1.5 \text{ m}\Omega \text{ cm}$) to the measured normal-state resistivity is less than unity and independent of field and sample. This result is in sharp contrast to the situation for high- T_c superconductors [14,15] where ρ_c is unphysically large (typically a few orders of magnitude larger than the normal-state resistivity). Finally, we note that near the transition onset regions of fluctuation superconductivity have dimension much less than the penetration depth, suggesting that dissipative flux creep, while dominant at lower temperatures, will not greatly interfere with the fluctuation conductivity contributions at the transition onset.

4.3. Upper-critical field and other normal and superconducting parameters

As discussed above, analysis of the magnetofluctuation conductivity near T_c allows $T_c(H)$ to be accurately

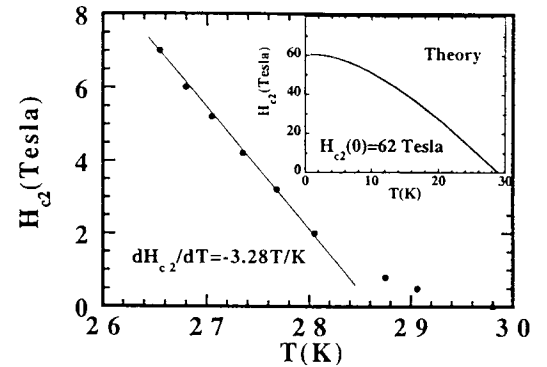


Fig. 4. $H_{c2}(T)$ vs. temperature. The solid line is a linear fit to the lower-temperature data with $dH_{c2}/dT = -3.28 \text{ T/K}$. The inset shows the theoretical curve of $H_{c2}(T)$ with the Pauli paramagnetic limiting, and the extrapolated value of $H_{c2}(0) = 62 \text{ T}$.

identified. From the T - H critical line, we obtain the upper critical field $H_{c2}(T)$ (Fig. 4). A linear fit to $H_{c2}(T)$ yields $dH_{c2}/dT = -3.28 \text{ T/K}$. The $H_{c2}(T)$ data have been analyzed in a manner similar to a previous study of K_3C_{60} [7] to extract the scattering time τ . This analysis makes a two square well approximation for the Eliashberg theory of the upper critical field. The fairly large value of $dH_{c2}/dT[1/(1 + \lambda)]$ for this material indicates the importance of Pauli limiting, which has been included in the analysis [17].

The treatment requires values for the Coulomb repulsion μ^* , the average phonon frequency $\bar{\omega}$, and the Fermi velocity v_F . The Coulomb repulsion is taken to be in the range $0.1 \leq \mu^* \leq 0.3$. The Fermi velocity can be approximated in two manners. A preliminary band-structure calculation for K_3C_{60} at the Rb_3C_{60} lattice constant yields $v_F \approx 1.56 \times 10^7 \text{ cm s}^{-1}$. This value is corroborated by a simple rescaling of the K_3C_{60} Fermi velocity by the ratio of the density of state for Rb and K doped C_{60} [18], which yields $v_F \approx 1.47 \times 10^7 \text{ cm s}^{-1}$. We take $v_F = 1.5 \times 10^7 \text{ cm s}^{-1}$. Estimates of the average phonon frequency are loosely based on three theoretical electron-phonon models of the superconducting properties of these materials [19–21]. The models of Jishi et al., Schluter et al., and Varma et al. are taken to have $\bar{\omega} \approx 500 \text{ K}$, 1000 K , 2000 K , respectively. Taking $\mu^* = 0.2$, we obtain $\tau \approx 5.5 \times 10^{-15} \text{ s}$ (Jishi), $\tau \approx 7 \times 10^{-15} \text{ s}$ (Schluter), $\tau \approx 7.5 \times 10^{-15} \text{ s}$ (Varma). Assuming $\mu^* = 0.1(0.3)$ produces scattering times roughly $1.0 \times 10^{-15} \text{ s}$ smaller (larger). Taking into account the uncertainties in the calculation, we estimate the zero-temperature scattering time of the

sample to be of the order $0.4\text{--}1.0 \times 10^{-14}$ s, implying a mean free path of $l = 11 \pm 5$ Å, several times the interatomic spacing. The extrapolated zero-temperature upper critical field is 62 T (see Fig. 4, inset), which yields a coherence length of $\xi(T=0) \approx 24$ Å. Since the coherence length is of the same order as the mean free path, Rb_3C_{60} is in neither the clean nor the dirty limit. For comparison, a treatment neglecting Pauli limiting would have yielded a critical field of 68 T. We note that a previous RF absorption measurement [5] on a Rb_3C_{60} powder sample under high field suggested that Pauli paramagnetic limiting may be significant, and a result of $H_{c2}(0) = 73$ T was obtained.

Knowledge of the scattering time and the plasma frequency ω_p allows one to make an estimation of the resistivity from the relation $\rho = (4\pi/\omega_p^2\tau)$. A preliminary band-structure estimate [22] yields a plasma frequency of 1.11 eV, close to the free electron value of 1.25 eV for three electrons of effective mass $3.6m_e$ per C_{60} (this value of the effective mass reproduces the band-structure Fermi velocity). This value is corroborated by reflectivity and electron energy loss measurements on K_3C_{60} , which is expected to have a comparable plasma frequency (theoretical estimates suggest a plasma frequency for K_3C_{60} rough 10% larger than that of Rb_3C_{60}). Infrared reflectivity measurements have been fit by a Drude model with a plasma frequency of 1.56 eV [23]. Electron energy loss spectroscopy measures the plasma frequency screened by the background dielectric constant of $\epsilon = 4.4$ [24]. These measurements yield a peak in the loss spectrum at 0.55 eV which corresponds to an unscreened plasma frequency of 1.15 eV [25]. For resistivity calculations, we use the theoretical value of $\omega_p = 1.11$ eV and the scattering time of $0.4\text{--}1.0 \times 10^{-14}$ s to obtain a zero-temperature resistivity of 0.57 ± 0.21 mΩ cm. This value compares well to theoretical calculations of 0.39 mΩ cm [26] and 0.42 mΩ cm [27] and infrared measurements of 0.7 mΩ cm [28]. The present result is slightly larger than estimates based on analysis of the fluctuation conductivity near T_c , which yield 0.23 mΩ cm.

Knowledge of ω_p , $\xi(0)$ and τ allows an estimation to be made of the penetration depth λ and the BCS coherence length ξ_0 within Ginzburg–Landau theory [29]. A plasma frequency of 1.11 eV implies a London penetration depth of $\lambda_L = e/\omega_p = 1690$ Å in the clean limit. Allowing for the finite value of τ within Ginz-

burg–Landau theory yields $\lambda(T=0) = 3200 \pm 800$ Å. Similarly, the experimental value for the zero-temperature coherence length, $\xi(0) = 24$ Å, together with $\tau \approx 0.4\text{--}1.0 \times 10^{-14}$ s yields a BCS clean-limit coherence length of $\xi_0 \approx 85 \pm 15$ Å. This value is somewhat larger than that obtained from Allen’s formula, $\xi_0 = [4\zeta(3)/7]^{1/2} h v_F / 2\pi [k_B T_c (1 + \lambda)]$, which yields $\xi_0 \approx 44 \pm 7$ Å for $\lambda \approx 0.7\text{--}1.3$, the relevant range for Rb_3C_{60} .

4.4. Low-field nonlinearity of H_{c2} data

We observe a deviation from the linear relation in H_{c2} data for fields of less than 2 T. A similar nonlinearity was also found for Rb_3C_{60} powder and K_3C_{60} powder and single-crystal samples [5,7,30]. The low-field tails are not likely due to the sample inhomogeneity because they are found in both 0D granular samples and 3D uniformly doped single crystal samples. This “foot” may be due to flux creep. Yeshurun and Malozemoff [9] pointed out that the large thermally activated flux creep in high- T_c materials would reduce the critical current J_c dramatically near the transition temperature, and this effect would suppress the measured T_c . A flux creep model predicts that $H_{c2} \sim (T_{co} - T)^{1.5}$. The best fitting of our low-field data versus temperature shows that $H_{c2} \sim (T_{co} - T)^{1.52}$ ($H < 2$ T), where $T_{co} = 29.8$ K. The agreement between experimental data and theory indicates that it is possible that flux creep plays an important role in the nonlinear behavior near T_c because of the low activation energy of flux creep in Rb_3C_{60} as discussed above.

Next we briefly consider using thermodynamic fluctuation as an explanation of the low-field “foot” in the H_{c2} data. Lobb [31] pointed out that at temperatures close to T_c the fluctuations of the order parameter become of the same order as the parameter itself. This causes the breakdown of the GL theory in the temperature range:

$$|T - T_c| < 1.07 \times 10^{-9} \{ (\kappa^4 T_{co}^3) / H_{c2}(0) \}, \quad (4)$$

where $\kappa = (\lambda_L / \xi(0))$. Within this range, $H_{c2}(T) \sim (T_{co} - T)^{1.34}$; a crossing over to the normal linear behavior will take place at lower temperatures. In conventional superconductors, the non-GL range is less than 10^{-6} K. For high- T_c materials, because of large value of κ and high T_c , the value of $|T - T_c|$ is roughly 0.1 K–1 K. For Rb_3C_{60} , the penetration depth λ_L of

Table 1
Superconducting state and normal-state parameters of Rb_3C_{60} and K_3C_{60} single crystals

Parameter	Rb_3C_{60} ^a	K_3C_{60} ^b
T_c	30 K	19.7 K
dH_{c2}/dT	-3.28 T/K	-1.34 T/K
$H_{c2}(0)$	62 T	17.5 T
$\xi(0)$	24 Å	45 Å
ξ_0	44 ± 7 Å ^c , 85 ± 15 Å ^d	96 ± 16 Å ^c , 130 ± 15 Å ^d
l	11 ± 5 Å	31 ± 7 Å
$\rho(T \rightarrow 0)$	0.57 ± 0.21 mΩ cm	0.18 ± 0.06 mΩ cm

^a This work.

^b Data from Ref. [11].

^c From Allen's formula.

^d From Ginzburg–Landau's formula.

about 3200 ± 800 Å, and coherence length of 24 Å implies a κ of roughly 100 to 150. Using $\kappa = 150$, $T_{c0} = 30$ K, $H_{c2}(0) = 62$ T gives $|T - T_c|$ in the order of 0.1 K. This value is somewhat less than we observed in the experiment.

5. Summary

In summary, the magnetoresistance properties of Rb_3C_{60} single crystal have been studied. We attribute the broadening of the resistive transition to the superconducting state to the combined effects of magneto-fluctuations near T_c and thermally activated flux creep at lower temperatures. Several normal and superconducting parameters were obtained from our analysis. Table 1 list the microscopic parameters characterizing the normal and superconducting states of single-crystal Rb_3C_{60} , together with corresponding parameters for single-crystal K_3C_{60} .

Acknowledgements

We thank W.A. Vareka, G. Briceno and B. Burk for valuable technical assistance, and thank S.C. Erwin for sharing theoretical results with us prior to publication. This research was supported by National Foundation grant DMR91-20269 and by the Office of Energy Research, Office of Basic Energy Sciences, Materials

Sciences Division of U.S. Department of Energy under contract DE-AC03-76SF00098. VHS was supported by a National Defence Science and Engineering Graduate Fellow.

References

- [1] A.F. Hebard et al., Nature (London) 350 (1991) 600; R.C. Haddon et al., Nature (London) 350 (1991) 320.
- [2] A.R. Kortan et al., Nature (London) 355 (1992) 529.
- [3] X.D. Xiang, J.G. Hou, V.H. Crespi, M.L. Cohen and A. Zettl, Nature (London) 361 (1993) 55.
- [4] G. Sparr et al., Phys. Rev. Lett. 68 (1992) 1228.
- [5] S. Foner et al., Phys. Rev. B 46 (1992) 14936.
- [6] C.E. Johnson, E.J. McNitt Jr., D. Heiman, S.-M. Huang and K.R. Kaner, Phys. Rev. B 46 (1992) 5880.
- [7] J.G. Hou et al., Solid State Commun. 86 (1993) 643.
- [8] S. Kambe et al., Physica C 160 (1989) 283.
- [9] Y. Yeshurum and A.P. Malozemoff, Phys. Rev. Lett. 60 (1988) 2202.
- [10] X.D. Xiang et al., Science 352 (1992) 1900.
- [11] K.D. Usadel, Phys. Lett. A 29 (1969) 50; K.D. Usadel, Z. Phys. 227 (1969) 260.
- [12] P.W. Anderson and Y.B. Kim, Rev. Mod. Phys. 36 (1964) 39.
- [13] M. Tinkham, Introduction to Superconductivity (McGraw-Hill, New York, 1975) p. 174.
- [14] T.T. Palstra et al., Phys. Rev. Lett. 61 (1988) 1662.
- [15] A.P. Malozemoff, B. Batlogg, L.F. Schneemeyer and J.V. Waszczak, Springer Series in Solid-State Sciences 89 (1989) 349 (Springer, Berlin, Heidelberg, 1989).
- [16] M. Tinkham, Phys. Rev. Lett. 61 (1988) 1658.
- [17] J.P. Carbotte, Rev. Mod. Phys. 62 (1990) 1102.
- [18] A. Oshiyami and S. Saito, Solid State Commun. 82 (1992) 41.
- [19] C.M. Varma, J. Zaanen and K. Raghavachari, Science 245 (1993) 989.
- [20] R.A. Jishi and M.S. Dresselhaus, Phys. Rev. B 45 (1992) 2597.
- [21] M. Schluter, M. Lannoo, M. Needles and G.A. Baraff, Phys. Rev. Lett. 68 (1992) 526.
- [22] S.C. Erwin, personal communication.
- [23] Y. Iwasa, K. Tanaka, T. Yasuda, T. Koda and S. Koda, Phys. Rev. Lett. 69 (1992) 2284.
- [24] A.F. Hebard, personal communication.
- [25] E. Sohmen, J. Fink and W. Kratschmer, Europhys. Lett. 17 (1992) 55.
- [26] M.P. Gelfand and J.P. Lu, Phys. Rev. B 46 (1992) 4367.
- [27] M.S. Deshpande, S.C. Erwin, S. Hong and E.J. Mele, Phys. Rev. Lett. 71 (1993) 2619.
- [28] L. Degiorgi et al., Phys. Rev. Lett. 69 (1992) 2897; L. Degiorgi et al., Phys. Rev. B 46 (1992) 11250.
- [29] N.R. Werthamer, Superconductivity, ed. R.D. Parks (M. Dekker, New York, 1969) p. 338.
- [30] K. Holczer et al., Phys. Rev. Lett. 67 (1991) 271.
- [31] C.J. Lobb, Phys. Rev. B 36 (1987) 3930.